

## Auger widths of core levels in metallic sodium and lithium

Arnold J. Glick and Amy Liu Hagen

*Department of Physics and Astronomy, University of Maryland, College Park, Maryland 20742*

(Received 12 January 1976; revised manuscript received 10 June 1976)

The Auger decay rates of the  $1s$  level in lithium and  $2p$  level in sodium are calculated using a diagrammatic many-body technique. The lowest-order nonvanishing contribution to the self-energy of these core states gives Auger widths of the order of  $10^{-3}$  eV for Li and  $10^{-4}$  eV for Na. However, higher-order terms are found to diverge showing that a renormalized theory must be used for such calculations. We find that for systems with low-lying excitations, there is a many-body mechanism which enhances the Auger width. Using a self-consistent renormalized theory, we find widths of the order of 20 meV for both Li and Na. The sodium result is consistent with predictions based on observed soft-x-ray spectra, but for lithium it is still one order of magnitude too small to be able to attribute the observed threshold behavior as purely due to an Auger core-level width.

### I. INTRODUCTION

Core-level spectroscopies have evoked much interest recently as probes of the electronic structure and surface composition of solids. Soft-x-ray emission and absorption, appearance-potential spectroscopy, x-ray photoemission, etc., make use of the spectra associated with electron transitions between a localized core state and the conduction band. In each case the assumption that the width of the core energy level is negligible simplifies the theoretical interpretation of the spectrum. However, there are features of the spectra, even for simple metals, which are difficult to explain without invoking a finite core lifetime. For example, Dow and co-workers<sup>1</sup> have stressed the importance of core width for explaining the threshold behavior of lithium soft-x-ray spectra. An effective core width can arise from processes such as phonon interactions and nonradiative (Auger) deexcitation. In this paper we reconsider Auger broadening and show that in systems with low-lying excitations there is a many-body mechanism which can enhance the Auger width. For sodium and lithium the width is increased by more than an order of magnitude over that found from a direct Auger calculation.

In 1940, Skinner<sup>2</sup> in his classic study of x-ray spectra proposed a natural core width of the order of  $10^{-2}$  eV for sodium and  $10^{-1}$  eV for lithium. These values were derived from the experimental spectra interpreted with a one-electron model of the transition. Later, McAlister<sup>3</sup> showed that the shape of both emission and absorption thresholds of lithium could be explained entirely in terms of one-electron band theory if a Gaussian broadening function were convoluted with the theoretical spectra. Ritsko *et al.*<sup>4</sup> determined the Gaussian broadening function by convoluting with a step discon-

tinuity at the threshold energy. Both estimated that the full width at half maximum of the  $1s$  level in lithium is about 0.5 eV. However, calculations of the Auger width to lowest order<sup>5</sup> give a width which is two orders too small to explain the lithium spectra.

An alternative approach was developed by Mahan<sup>6</sup> and by Nozières and co-workers<sup>7</sup> who studied many-body effects on the x-ray spectra. Nozières and de Dominicis<sup>8</sup> (ND) considered the effect of switching on or off the localized core-hole potential and found that perturbation theory was inadequate to describe the process. A nonperturbative solution valid near the threshold but neglecting lifetime effects showed that the x-ray intensity was enhanced for  $L$  spectra and was diminished for  $K$  spectra at the threshold. These results are qualitatively correct.<sup>9</sup> But the falloff of the Li spectrum is not so rapid as the many-body theory suggests.

The ND theory is only valid very close to the threshold. Longe<sup>10</sup> used a first-order theory to study the ND effect away from the edge and found that the edge singularity was not strong enough to explain the premature peak observed in the emission  $K$  bands of Li and Be. He suggested that the  $p$ -scattering resonance discussed by Allotey<sup>11</sup> was the dominant factor. Mahan<sup>12</sup> suggested that the ND theory could be extended over the whole spectrum by means of a convolution with a broadening function, and that the Li data could be fit if the core width was on the order of 0.2–0.3 eV. However, his theory leaves out conduction-electron lifetimes which are important away from the edge.<sup>13–15</sup>

Dow *et al.*<sup>1</sup> claimed that the Li threshold behavior can be attributed to an indirect interaction of the  $1s$  core level with the lattice which gives the core an effective width of 0.46 eV. Bergersen *et*

*al.*<sup>5</sup> questioned their result, claiming that the Dow process is no different than the direct interaction of the core level with the lattice vibration. The latter process<sup>16</sup> gives an insufficient width of the order of 50 meV at zero temperature for Li and Na. They attributed the larger width found by Dow *et al.* to an overestimation of the amplitude of the local dilation and compression fluctuations. He-din<sup>17</sup> in a recent recalculation of the phonon effect claims that there is an enhancement due to Friedel oscillations in the electron-phonon interaction. Using an Ashcroft-type pseudopotential, he finds temperature-dependent widths on the order of tenths of an electronvolt.

Franceschetti and Dow<sup>18</sup> calculated the Auger width for atomic Li and found that orbital relaxation could enhance the width by a factor of 16. They proposed that this effect could also enhance the Auger width for metallic Li. We used a simple model to study the Auger widths for atomic Li and Na and found similar results to theirs.<sup>19</sup> However, when we apply the same technique to the metallic cases, the Auger widths for both metallic Li and Na are not appreciably affected by orbital relaxation.

In summary it appears that there is still no generally accepted explanation for the core-level widths inferred from observed soft-x-ray spectra. In the present paper we consider the nonradiative or Auger width of the core level and go beyond the lowest-order calculations of Bergersen *et al.*<sup>5</sup> and Kobayashi and Morita.<sup>20</sup> We use a Feynman diagrammatic technique to calculate the self-energies of the 1s level in Li and 2p level in Na. The lowest-order contribution to the imaginary part of the self-energy is found to depend strongly on the behavior of the conduction-electron wave function in the neighborhood of the core hole. We then proceed to a higher-order graph and find it to be divergent. Thus perturbation theory is not valid and a renormalized theory is necessary. A renormalized core-hole propagator is introduced which in itself depends on the lifetime which we are trying

to calculate. Treating the half-width as a parameter, we seek a self-consistent solution and find an enhanced width of 20 meV for both Li and Na. Section IV contains a discussion of the results and summary.

## II. LOWEST-ORDER CALCULATIONS

The half-width of the core state is simply related to the imaginary part of its self-energy evaluated on the energy shell

$$\Gamma = \text{Im}\Sigma(\omega_B), \quad (1)$$

where  $\omega_B$  contains the shift from the unperturbed energy  $E_B$  due to the real part of the self-energy, i.e.,  $\omega_B$  is the solution of

$$\omega_B = E_B + \text{Re}\Sigma(\omega_B). \quad (2)$$

In terms of Feynman-type diagrams, the lowest-order nonradiative contributions to the self-energy are shown in Figs. 1(a)–1(c). The dashed lines represent Coulomb interaction between electrons. Upward-directed single lines represent conduction electrons in states above the Fermi level and downward single lines represent holes in the filled portion of the conduction band. A downward-directed double line represents a hole in the localized core level whose self-energy we are attempting to calculate.

Figure 1(a) represents the excitation of a particle-hole pair due to polarization of the electron gas by the core hole. However, it is usually argued that since the core hole does not change energy in the transition to the intermediate state, energy can not be conserved. Thus this graph represents a virtual process which can give rise to an energy shift, but not to a lifetime. We will reconsider this argument in Sec. III.

Figure 1(b) is the usual Auger process and Fig. 1(c) is an exchange term which differs in sign and lacks a factor of 2 which enters the direct term due to spin. These two terms give rise to a core-state self-energy  $\Sigma_{bc}(\omega)$ :

$$\begin{aligned} \Sigma_{bc}(\omega) = & -\frac{i}{l} \sum_j \sum_{\vec{k}_1} \sum_{\vec{k}_2} \sum_{\vec{k}_v} \int \frac{d\omega_1}{2\pi i} \frac{d\omega_v}{2\pi i} v(\vec{k}_v) f_j(\vec{k}_2, -\vec{k}_v) [2v(\vec{k}_v) f_j(\vec{k}_2, -\vec{k}_v) - v(\vec{k}_1 + \vec{k}_v - \vec{k}_2) f_j(\vec{k}_1, -\vec{k}_1 - \vec{k}_v + \vec{k}_2)] \\ & \times G(\vec{k}_2, \omega_v + \omega) G(\vec{k}_1, \omega_1) G(\vec{k}_1 + \vec{k}_v, \omega_1 + \omega_v), \end{aligned} \quad (3)$$

where the vertex function

$$f_j(\vec{k}_a, \vec{k}_v) = \langle u_j^B(\vec{r}) | e^{i\vec{k}_v \cdot \vec{r}} | u_{\vec{k}_a}(\vec{r}) \rangle \quad (4)$$

represents a transition from a conduction state of momentum  $\vec{k}_a$  to a core state which is  $l$ -fold degenerate.  $j$  is a degeneracy index ( $j = 1, 2, 3$  for the 2p state and we neglect spin-orbit splitting). The

core wave functions were constructed using Slater's rules.<sup>21</sup> Three sets of conduction states were considered in evaluating Eq. (4): (i) simple plane waves, (ii) plane waves orthogonalized to the core states, and (iii) plane waves orthogonalized to a relaxed set of core states; i.e., core states constructed to account for the reduction in screening

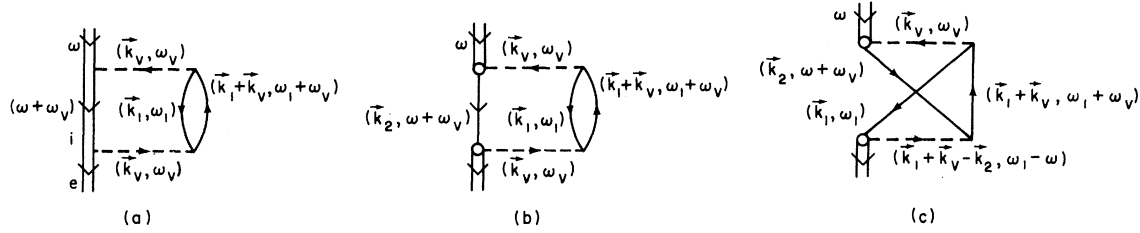


FIG. 1. Core-state self-energy diagrams: (a) lowest order; (b) Auger self-energy; (c) exchange graph.

when one core electron is absent. The appendix contains explicit expressions for the wave functions and matrix elements. For  $v(\vec{k})$ , the electron-electron interaction, we used a Thomas-Fermi screened Coulomb potential.  $G(\vec{k}, \omega)$  is a bare propagator for a conduction electron in a state of momentum  $\vec{k}$  and energy  $E_k = k^2/2m$ :

$$G(\vec{k}, \omega) = \frac{i\eta_{\vec{k}>}}{\omega - E_{\vec{k}} + i\lambda} + \frac{i\eta_{\vec{k}<}}{\omega - E_{\vec{k}} - i\lambda}, \quad (5)$$

where

$$\Sigma_a(\omega) = -\frac{2i}{l} \sum_{e,j} \sum_{\vec{k}_1} \sum_{\vec{k}_v} \int \frac{d\omega_1}{2\pi i} \int \frac{d\omega_2}{2\pi i} |v(\vec{k}_v) g_{e,j}(\vec{k}_v)|^2 G_B(\omega + \omega_2) G(\vec{k}_1, \omega_1) G(\vec{k}_1 + \vec{k}_v, \omega + \omega_2), \quad (6)$$

where

$$g_{e,j}(\vec{k}_v) = \langle u_j^B(\vec{r}) | e^{i\vec{k}_v \cdot \vec{r}} | u_e^B(\vec{r}) \rangle \quad (7)$$

is a core-core vertex function and

$$G_B(\omega) = i/(\omega - E_B - i\lambda)$$

is the bare core-state propagator, where  $E_B (<0)$  is the unperturbed core-state energy. The matrix

$$\Sigma_a(\omega) = -\frac{2}{l} \sum_{e,j} \sum_{\vec{k}_1} \sum_{\vec{k}_v} \eta_{\vec{k}_1 <} \eta_{\vec{k}_1 + \vec{k}_v >} |v(\vec{k}_v) g_{e,j}(\vec{k}_v)|^2 \frac{1}{E_B - \omega + E_{\vec{k}_1} - E_{\vec{k}_1 + \vec{k}_v} + i\lambda}. \quad (8)$$

The real part and the imaginary part of the self-energy are then

$$\text{Re}\Sigma_a(\omega) = -\frac{2}{l} \sum_{e,j} \sum_{\vec{k}_1} \sum_{\vec{k}_v} \eta_{\vec{k}_1 <} \eta_{\vec{k}_1 + \vec{k}_v >} |v(\vec{k}_v) g_{e,j}(\vec{k}_v)|^2 \frac{1}{E_B - \omega + E_{\vec{k}_1} - E_{\vec{k}_1 + \vec{k}_v}}, \quad (9)$$

and

$$\text{Im}\Sigma_a(\omega) = \frac{2\pi}{l} \sum_{e,j} \sum_{\vec{k}_1} \sum_{\vec{k}_v} \eta_{\vec{k}_1 <} \eta_{\vec{k}_1 + \vec{k}_v >} |v(\vec{k}_v) g_{e,j}(\vec{k}_v)|^2 \delta(E_{\vec{k}_1} + E_B - \omega - E_{\vec{k}_1 + \vec{k}_v}). \quad (10)$$

Equation (9) was evaluated numerically as a function of frequency with the aid of the UNIVAC 1108 computer of the University of Maryland. The results are summarized in Figs. 2 and 3. A simple

$$\eta_{\vec{k}<} = \begin{cases} 1 & \text{if } |\vec{k}| < \vec{k}_F, \\ 0 & \text{otherwise} \end{cases}$$

and

$$\eta_{\vec{k}>} = 1 - \eta_{\vec{k}<}$$

is an infinitesimal positive number.

To find the lifetime resulting from these graphs we must evaluate  $\Sigma_{bc}(\omega)$  on the energy shell  $\omega = \omega_B$  where  $\omega_B$  is determined from Eq. (2). To find  $\omega_B$  we need the complete self-energy. Now Fig. 1(a) cannot be neglected. Its contribution to the self-energy is

elements  $g_{e,j}(\vec{k}_v)$  and  $f_j(\vec{k}_a, \vec{k}_v)$  are given in the Appendix. For both lithium and sodium one finds that the  $g_{e,j}(\vec{k}_v)$  are much larger than the  $f_j(\vec{k}_a, \vec{k}_v)$  due to poor overlap of conduction and core wave functions. Consequently the contribution from Fig. 1(a) is larger by a factor of  $10^3$  than those from Figs. 1(b) and 1(c). After integrating over frequencies, Eq. (6) becomes

graphical method can be used to find the root of equation  $\omega = E_B + \text{Re}\Sigma_a(\omega)$ . In Figs. 2 and 3,  $\eta = \text{Re}\Sigma_a(\omega)$  is plotted as a function of  $(\omega - E_B)$  for the case of lithium and sodium, respectively. The re-

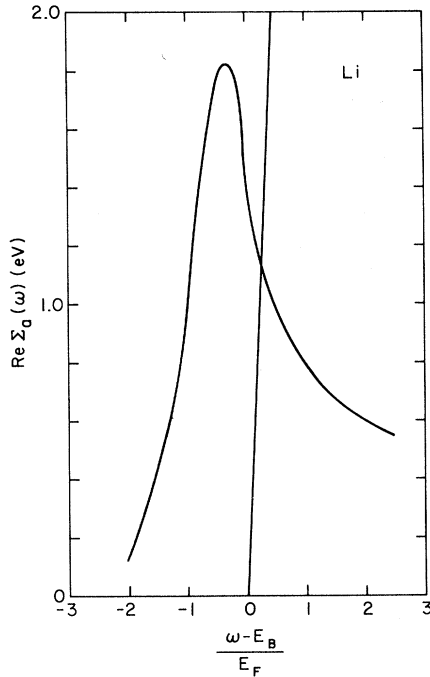


FIG. 2. Real part of the core self-energy due to Fig. 1(a) plotted against frequency for Li. Intersection of the  $\text{Re}\Sigma$  curve and the straight line gives the solution of the equation  $\omega = E_B + \text{Re}\Sigma(\omega)$ .

normalized bound-state energy  $\omega_B$  is found by determining the point of intersection of this curve with the curve  $\eta = \omega - E_B$ .

The final results are

$$\begin{aligned} \text{Re}\Sigma_a(\omega_B) &= 1.14 \text{ eV}, \\ \text{Re}\Sigma_a(\omega_B) &= 0.88 \text{ eV}. \end{aligned} \quad (11)$$

$$\begin{aligned} \text{Im}\Sigma_{bc}(\omega) &= \frac{\pi}{l} \sum_j \sum_{\vec{k}_1} \sum_{\vec{k}_2} \sum_{\vec{k}_v} v(\vec{k}_v) f_j(\vec{k}_2, -\vec{k}_v) [2v(\vec{k}_v) f_j(\vec{k}_2, -\vec{k}_v) - v(\vec{k}_1 + \vec{k}_v - \vec{k}_2) f_j(\vec{k}_1, -\vec{k}_1 - \vec{k}_v + \vec{k}_2)] \\ &\quad \times [\eta_{\vec{k}_2} \langle \eta_{\vec{k}_1} \rangle \eta_{\vec{k}_1 + \vec{k}_v} \delta(E_{\vec{k}_2} + E_{\vec{k}_1} - E_{\vec{k}_1 + \vec{k}_v} - \omega) + \eta_{\vec{k}_2} \langle \eta_{\vec{k}_1} \rangle \eta_{\vec{k}_1 + \vec{k}_v} \delta(E_{\vec{k}_1 + \vec{k}_v} - E_{\vec{k}_1} - E_{\vec{k}_2} + \omega)]. \end{aligned} \quad (13)$$

When  $\omega = \omega_B$ , the second  $\delta$  function of Eq. (13) can not be satisfied. Evaluating the surviving term using a Monte-Carlo method one finds the results shown in Table I. It is seen that the results are sensitive to the choice of conduction-electron wave functions. The orthogonalized and relaxed wave functions are expected to be the most accurate, and they give

$$\begin{aligned} \text{Im}\Sigma_{bc}(-30.28 \text{ eV}) &= 0.67 \times 10^{-4} \text{ eV for Na}, \\ \text{Im}\Sigma_{bc}(-53.18 \text{ eV}) &= 0.90 \times 10^{-3} \text{ eV for Li}. \end{aligned} \quad (14)$$

Note that the imaginary part of the self-energy

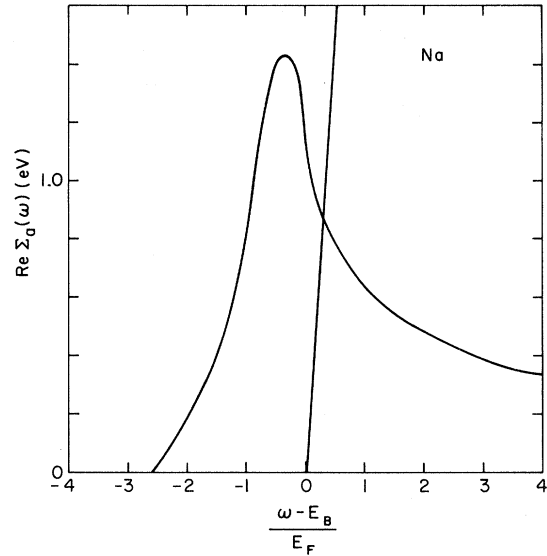


FIG. 3. Real part of the core self-energy due to Fig. 1(a) plotted against frequency for Na. Intersection of the  $\text{Re}\Sigma$  curve and the straight line gives the solution to the equation  $\omega = E_B + \text{Re}\Sigma(\omega)$ .

Thus the renormalized bound-state energies are

$$\begin{aligned} \omega_B &= -53.18 \text{ eV for Li}, \\ \omega_B &= -30.28 \text{ eV for Na}. \end{aligned} \quad (12)$$

The corresponding Auger width of the core level is given by the imaginary part of Eq. (3). After integrating over frequencies and selecting out the imaginary part, Eq. (3) gives

gives the half width of the core state. Twice this value gives the full width which can be compared with results quoted elsewhere. If the orthogonalization of the plane wave to the core states is neglected, then one finds widths which are in agreement with those found in Refs. 5 and 20 and are of the order of  $10^{-3}$  eV for both lithium and sodium. Orthogonalization reduces the lithium width by a factor of 0.7, as has also been noted in Ref. 5. For sodium the reduction factor is much more dramatic. In contrast with the prediction by Franceschetti and Dow and the findings for atomic Auger processes,<sup>18,19</sup> relaxation of the wave functions has

TABLE I. Auger half-width of the core levels in sodium ( $2p$  state) and lithium ( $1s$  state) for different choices of conduction-electron wave functions used in Eq. (4).

Wave function		$\Gamma_0$ (eV) = $\text{Im}\Sigma_{bc}(\omega_B)$	
Orthogonalized	Relaxed	Na	Li
Yes	Yes	$0.67 \times 10^{-4}$	$0.90 \times 10^{-3}$
Yes	No	$0.44 \times 10^{-4}$	$0.16 \times 10^{-2}$
No	No	$0.13 \times 10^{-2}$	$0.23 \times 10^{-2}$

a much weaker effect. Indeed, even the direction of the relaxation effect is not apparent *a priori*. Relaxation broadens the sodium level but narrows the level in lithium. These results can be understood by noting that  $k_v$  is restricted by the  $\delta$  function in Eq. (3) to take values two or three times the Fermi wave number. The oscillations of the conduction wave function in the core region, accounted for by the orthogonalization terms, reduce the matrix element significantly, but small changes in the phase of the oscillation introduced by relaxation apparently have little effect when  $k_v$  is so large. For the atomic case where  $k_1$  and  $k_2$  are replaced by localized levels,  $k_v$  is not restricted to large values. [Note that here we can neglect orthogonalization corrections to conduction-electron-conduction-electron vertices since such corrections are of higher order in the vertex functions  $f_j(\vec{k}_a, \vec{k}_b)$  and are small.]

$$\Sigma_{4d}(\omega) = \frac{4i}{l} \sum_{e,j} \sum_{\vec{k}_1} \sum_{\vec{k}_3} \sum_{\vec{k}_v} \sum_{\vec{q}} \sum_{\vec{k}_2} \int \frac{d\omega_1}{2\pi i} \int \frac{d\omega_3}{2\pi i} \int \frac{d\omega_v}{2\pi i} \int \frac{d\Omega}{2\pi i} G(\vec{k}_1, \omega_1) G(\vec{k}_1 + \vec{k}_v, \omega_1 + \omega_v) \\ \times G(\vec{k}_3, \omega_3) G(\vec{k}_3 + \vec{q}, \omega_3 + \Omega) G(\vec{k}_2, \omega + \Omega + \omega_v) [G_B(\omega + \Omega)]^2 \\ \times |g_{e,j}(\vec{q}) f_j(\vec{k}_v, -\vec{k}_2)|^2 |v(\vec{q})v(\vec{k}_v)|^2. \quad (15)$$

After integrating over frequencies,

$$\text{Im}\Sigma_{4d}(\omega_B) = \frac{4}{l} \sum_{e,j} \sum_{\vec{k}_1} \sum_{\vec{k}_3} \sum_{\vec{k}_v} \sum_{\vec{q}} \sum_{\vec{k}_2} \eta_{\vec{k}_1 < \vec{k}_1 + \vec{k}_v} \eta_{\vec{k}_3 < \vec{k}_3 + \vec{q}} \eta_{\vec{k}_2 < \vec{k}_2 + \omega + \Omega + \omega_v} |g_{e,j}(\vec{q}) f_j(\vec{k}_v, -\vec{k}_2) v(\vec{q}) v(\vec{k}_v)|^2 \\ \times \frac{\delta(E_B + E_{\vec{k}_3 + \vec{q}} + E_{\vec{k}_1 + \vec{k}_v} - E_{\vec{k}_1} - E_{\vec{k}_3} - E_{\vec{k}_2})}{(E_{\vec{k}_3 + \vec{q}} - E_{\vec{k}_3})^2}. \quad (16)$$

The integral in Eq. (16) is divergent for  $E_{\vec{k}_3 + \vec{q}} \approx E_{\vec{k}_3}$ . Thus perturbation theory is not valid. To incorporate such terms completely in the calculation it would appear to be necessary to use a theory analogous to that of Nozières and de Dominicis.<sup>8</sup> Natta and Joyes<sup>22</sup> studied the Auger process from this point of view, but in their solution, as well as the ND solution for the soft-x-ray case, one only obtains an asymptotically valid solution for a threshold energy, here equivalent to  $E_{\vec{k}_2} = E_F$ , the Fermi energy. In Eqs. (13) and (16) an integral

in x-ray emission and absorption, certain higher-order graphs are singular and have a strong effect on the shape of the spectrum. There are higher-order Auger graphs which have a structure similar to those graphs. We now show that in the next order there is a term of this type which diverges, showing that the Auger calculation presented above is not complete. Then we will be led to a renormalized calculation which gives an enhanced Auger width.

### III. HIGHER-ORDER DIVERGENCE AND SELF-CONSISTENT CALCULATION

Singularities in core-level spectroscopy arise as a transient response to the disappearance of the impurity-like potential associated with the core hole. Low-energy electron-hole pairs are created virtually by scattering off the localized potential. When a conduction electron falls into the core state the potential disappears and the electron-hole pairs are left in real excited states. If sufficient phase space is available these excitations can give rise to peaks in the spectra. This mechanism is the source of the threshold singularities in soft x-ray spectra.<sup>6, 7, 14</sup> Analogous terms which can contribute to the Auger width are shown in Fig. 4. Through fourth order in the Coulomb interaction, only Fig. 4(d) exhibits a divergence of this type.

Applying Feynman's rules the contribution of this graph is

over  $E_{\vec{k}_2}$  is required.

Rather than attempt a full solution to the ND problem we note that Fig. 4(d) can be viewed in two ways. Above we considered it to be a correction to Fig. 1(b). It can also be viewed as a correction to Fig. 1(a), in which the intermediate-bound-state propagator has a self-energy insertion. When the self-energy of the core state is taken into account this term's contribution to the Auger width no longer vanishes, indeed it is singular. Thus perturbation theory is not valid and a

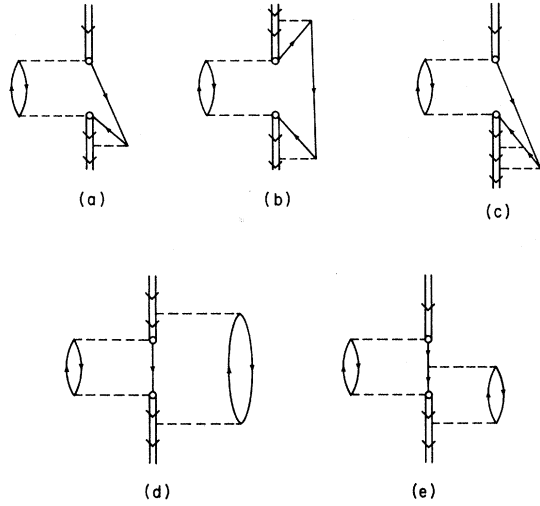


FIG. 4. Selected higher-order terms contributing to the Auger width. All of these graphs contain electron-hole pair creation due to scattering by the core hole. Graph (d) gives a divergent contribution.

renormalized theory is necessary. We therefore sum all self-energy processes as shown in Fig. 5. This procedure is equivalent to recalculating the contribution to the self-energy from the lowest-order graph as shown in Fig. 1(a) except that now the core-state propagator contains a self-energy which we denote by  $\text{Re}\Sigma^B(\omega) + i\Gamma$ :

$$G_B^R(\omega) = \frac{i}{\omega - E_B - \text{Re}\Sigma^B(\omega) - i\Gamma} \approx \frac{i}{\omega - \omega_B - i\Gamma}, \quad (17)$$

where  $\omega_B = E_B + \text{Re}\Sigma_a^B(\omega_B)$  and  $\Gamma$  is treated as a parameter. Similar to Eq. (10) we have now

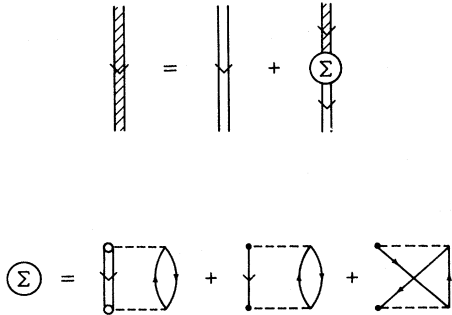


FIG. 5. Schematic representation of the Dyson's equation satisfied by the renormalized core propagator. Double shaded line represents the renormalized core-hole propagator. Double line without shading represents the noninteracting propagator.  $\Sigma$  represents the sum of all proper self-energy parts, of which the lowest-order terms are shown.

$$\begin{aligned} \text{Im}\Sigma_a^{RB}(\omega, \Gamma) &= \frac{2\pi}{l} \sum_{e,j} \sum_{\vec{k}_1, \vec{k}_v} \eta_{\vec{k}_1} \langle \eta_{\vec{k}_1 + \vec{k}_v} \rangle |v(\vec{k}_v) g_{ej}(\vec{k}_v)|^2 \\ &\quad \times \frac{\Gamma}{(\omega_B - \omega + E_{\vec{k}_1} - E_{\vec{k}_1 + \vec{k}_v})^2 + \Gamma^2}, \end{aligned} \quad (18)$$

when  $\omega = \omega_B$ ,

$$\begin{aligned} \text{Im}\Sigma_a^{RB}(\omega_B, \Gamma) &= \frac{2\pi}{l} \sum_{e,j} \sum_{\vec{k}_1, \vec{k}_v} \eta_{\vec{k}_1} \langle \eta_{\vec{k}_1 + \vec{k}_v} \rangle |v(\vec{k}_v) g_{ej}(\vec{k}_v)|^2 \\ &\quad \times \frac{\Gamma}{(E_{\vec{k}_1 + \vec{k}_v} - E_{\vec{k}_1})^2 + \Gamma^2}. \end{aligned} \quad (19)$$

We evaluate  $\text{Im}\Sigma_a^{RB}$  as a function of  $\Gamma$  and then require self-consistency so that  $\Gamma$  is obtained from the equation

$$\Gamma = \Gamma_0 + \text{Im}\Sigma_a^{RB}(\omega_B, \Gamma), \quad (20)$$

where  $\Gamma_0 = \text{Im}\Sigma_{bc}(\omega_B)$ .

The final expressions for  $\text{Im}\Sigma_a^{RB}$  for Li and Na were obtained by numerical calculations and are plotted in Figs. 6 and 7. By solving Eq. (20)

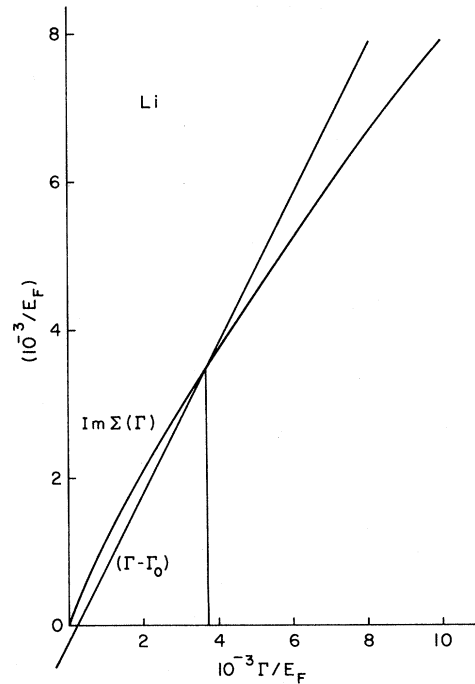


FIG. 6. Imaginary part of the core self-energy due to Fig. 1(a) with renormalized core propagator, plotted against  $\Gamma$  for Li. Intersection of the  $\text{Im}\Sigma$  curve and the straight line gives the solution of the equation  $\Gamma = \Gamma_0 + \text{Im}\Sigma$ , where  $\Gamma_0 = \text{Im}\Sigma_{bc}^B(\omega_B)$ .

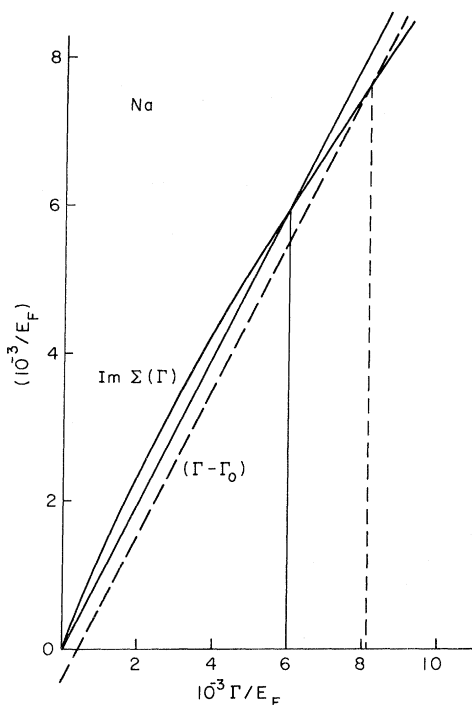


FIG. 7. Imaginary part of the core self-energy due to Fig. 1(a) with renormalized core propagator, plotted against  $\Gamma$  for Na. Intersection of the  $\text{Im}\Sigma$  curve and the straight line gives the solution to the equation  $\Gamma = \Gamma_0 + \text{Im}\Sigma$ , where  $\Gamma_0 = \text{Im}\Sigma_{bc}^B(\omega_B)$ . Straight solid line is  $\Gamma_0$  calculated using orthogonalized and relaxed conduction-electron wave functions. Dashed line is  $\Gamma_0$  calculated with simple free-electron wave functions.

graphically, we find that:

$$\begin{aligned} \Gamma &= 0.37 \times 10^{-2} E_F = 17 \text{ meV} \text{ for Li,} \\ \Gamma &= 0.60 \times 10^{-2} E_F = 19 \text{ meV} \text{ for Na,} \end{aligned} \quad (21)$$

where we have used  $E_F = 4.7$  eV for Li and  $E_F = 3.1$  eV for Na. These results are not very sensitive to  $\Gamma_0$ . In the case of sodium, where the difference between the calculated values of  $\Gamma_0$  with and without orthogonalized wave functions is so large (see Table I), neglect of orthogonalization would shift the  $\Gamma - \Gamma_0$  curve to the dashed line in Fig. 7. Our result for  $\Gamma$  with this omission is  $\Gamma = 0.81 \times 10^{-2} E_F = 25$  meV. Thus the renormalization theory gives a level half-width which is one order larger than previously found for lithium and several orders larger than the best Auger value for sodium. For both materials we find half-widths on the order of 20 meV.

#### IV. CONCLUSIONS

As noted in Sec. I, the rounded thresholds of soft-x-ray absorption and emission spectra suggest

that the linewidth of the 1s level in Li is about 0.5 eV. We evaluated the contribution of the Auger decay rate to the core-level width of Li. In the meantime, we calculated the Auger rate for the 2p level of Na for the purpose of comparison. Soft-x-ray spectra indicate that L-shell widths are an order of magnitude smaller than comparable K widths.

The lowest-order diagram as shown in Fig. 1(a) contributed a small correction to the bound-state energy, however it didn't give any contribution to the imaginary part of the self-energy. Then we calculated the other lowest-order graphs as shown in Figs. 1(b) and 1(c) and found half-widths that are smaller by three orders of magnitude than the experimentally inferred values for both Li and Na. We then considered higher-order graphs and found some terms to be singular. Perturbation theory is therefore not valid. Returning to the lowest-order graph shown in Fig. 1(a) we introduced a renormalized core-hole propagator to account for the instability of the system to low-energy particle-hole creation. The half-width  $\Gamma$  was treated as a parameter to be determined self-consistently from the equation  $\Gamma = \Gamma_0 + \text{Im}\Sigma(\Gamma)$ . In this way  $\Gamma$  was found to be  $1.7 \times 10^{-2}$  eV for Li and  $1.9 \times 10^{-2}$  eV for Na. Thus this calculation does not account for the observed *difference* between the threshold widths of K and L spectra. For Na, the result is consistent with observed x-ray spectra. However, for Li it is still one order less than would be necessary to explain the soft-x-ray anomalies.

In our calculation we neglected vertex corrections except insofar as the use of relaxed wave functions is equivalent to introducing a vertex renormalization. In the ND theory of x-ray thresholds<sup>8,9</sup> the vertex plays a crucial role in distinguishing K and L spectra. For the x-ray case the relevant operator causing the transition is the electric dipole moment. For the Auger width it is the full exponential operator which mixes partial waves and hence washes out symmetry differences. Thus vertex corrections are not expected to change the conclusion that calculated Auger widths are of the same order of magnitude for s and p core states in light metals. As a consequence, it appears unlikely that a difference of Auger width is the source of the observed differences between K and L soft-x-ray spectra.

#### ACKNOWLEDGMENTS

The computer time for this project was supported in full through the facilities of the Computer Science Center of the University of Maryland. One of us (A.J.G.) would like to thank the Aspen Center for Physics for hospitality during part of the tim

that this work was being carried out and R. Prange for interesting discussions.

#### APPENDIX: VERTEX CONTRIBUTIONS $f_i(\vec{k}, \vec{q})$ AND $g_{ij}(\vec{q})$

##### A. Sodium

The core wave functions are the same as used previously.<sup>14</sup> They are constructed from hydrogenic-type functions with parameters determined according to Slater's rules<sup>21</sup> and orthonormalized:

$$u_{1s}^B(\vec{r}) = (\alpha^3/\pi)^{1/2} e^{-\alpha r}, \quad (\text{A1a})$$

$$u_{2s}^B(\vec{r}) = \frac{(\alpha + \beta)^4}{(4\pi D)^{1/2}} r e^{-\beta r} - \frac{3(2\alpha)^3}{(4\pi D)^{1/2}} e^{-\alpha r}, \quad (\text{A1b})$$

$$u_{2p, i}^B(\vec{r}) = (\beta^5/\pi)^{1/2} (x_i/r) r e^{-\beta r}, \quad i = 1, 2, 3, \quad (\text{A1c})$$

where  $r = (x_1^2 + x_2^2 + x_3^2)^{1/2}$  and  $D = 3(\alpha + \beta)^3/4\beta^5 - 18(2\alpha)^3$ . The parameters  $\alpha$  and  $\beta$  depend on the actual charge  $Z$  on the nucleus and the screening  $s$  by electrons in shells within and up to the one being considered. For sodium with both electrons in the shell, a 1s electron has shielding parameter  $\alpha = (Z - s)/n^*$ , where  $n^* = 1$  is the effective principal quantum number,  $Z = 11$  for sodium and  $s = 0.30$ , giving  $\alpha = 11 - 0.30 = 10.70$  in units of reciprocal Bohr radii  $a_0^{-1}$ . For the 2s and 2p states  $n^* = 2$  and  $s = 0.85 \times 2 + 0.35 \times 7 = 4.15$  due to screening by two electrons in the 1s state and seven others in the  $n = 2$  shell. Then  $\beta = \frac{1}{2}(11 - 4.15) = 3.425$ . The conduction-electron wave functions are taken

to be plane waves orthogonalized to relaxed core states. They can be written in the form

$$u_k(\vec{r}) = e^{i\vec{k}\cdot\vec{r}} - A_k^* e^{-\alpha^* r} - B_k^* r e^{-\beta^* r} - C_k^* \sum_{i=1}^3 k_i x_i e^{-\beta^* r}, \quad (\text{A2})$$

where

$$A_k^* = 8\alpha^{*4}/(\alpha^{*2} + k^2)^2 - 18(M_k^*/N^*)(2\alpha^*)^3,$$

$$B_k^* = 6M_k^*/N^*(\alpha^* + \beta^*)^4,$$

$$C_k^* = 32\beta^{*6}/(k^2 + \beta^{*2})^3$$

and

$$M_k^* = (\alpha^* + \beta^*)^4 (3\beta^{*2} - k^2)/3(\beta^{*2} + k^2)^3 - 8\alpha^{*4}/(\alpha^{*2} + k^2)^2,$$

$$N^* = 3(\alpha^* + \beta^*)^6/4\beta^{*5} - 18(2\alpha^*)^3.$$

The asterisks on  $\alpha^*$  and  $\beta^*$  and on the quantities which depend on  $\alpha^*$  and  $\beta^*$  allow for the difference in screening when one core state is unoccupied, as would be the case for the Auger initial state.

Since we are only considering the  $L_{23}$  spectrum of sodium,  $\alpha^* = \alpha$  is unaffected by a hole in a shell which is further out. However, states in the second shell are affected. Now

$$\beta^* = \frac{1}{2}(11 - 0.85 \times 2 - 0.35 \times 6) = 3.6.$$

The vertex contributions can now be evaluated:

$$f_i(\vec{k}, \vec{q}) = \langle u_{2p, i}^B(\vec{r}) | e^{i\vec{q}\cdot\vec{r}} | u_{\vec{k}}^B(\vec{r}) \rangle$$

$$= 32(\pi\beta^5)^{1/2} \left( \frac{\beta(k_i + q_i)}{(|\vec{k} + \vec{q}|^2 + \beta^2)^3} - \frac{A_k^*(\alpha^* + \beta^*)q_i}{[(\alpha^* + \beta)^2 + q^2]^3} - \frac{B_k^*[5(\beta + \beta^*)^2 - q^2]q_i + C_k^*(\beta + \beta^*)}{[q^2 + (\beta + \beta^*)^2]^4} \frac{6q_i(\vec{k} \cdot \vec{q}) - k_i[q^2 + (\beta + \beta^*)^2]}{[q^2 + (\beta + \beta^*)^2]^4} \right). \quad (\text{A3})$$

For the bound-bound matrix element  $g_{ij}(\vec{q})$  of Eq. (7), the initial core state is associated with one less screening electron. Thus with relaxation taken into account

$$g_{ij}(\vec{q}) = \langle u_{2p, i}^B(\vec{r}) | e^{i\vec{q}\cdot\vec{r}} | u_{2p, j}^B(\vec{r}) \rangle = 32(\beta\beta^*)^{5/2}(\beta + \beta^*) \left( \frac{\delta_{ij}}{[q^2 + (\beta + \beta^*)^2]^3} - \frac{6q_i q_j}{[q^2 + (\beta + \beta^*)^2]^4} \right). \quad (\text{A4})$$

Calculations were performed (a) with orthogonalized and relaxed wave functions as listed above, (b) by neglecting relaxation (setting  $\beta^* = \beta = 3.425$ ), and (c) without orthogonalization or relaxation (setting  $A_k^* = B_k^* = C_k^* = 0$ ).

##### B. Lithium

In this case there is only one core wave function

$$u_{1s}^B(\vec{r}) = (\alpha^3/\pi)^{1/2} e^{-\alpha r} \quad (\text{A5})$$

and the corresponding orthogonalized plane wave is

$$u_{\vec{k}}(\vec{r}) = e^{i\vec{k}\cdot\vec{r}} - [8\alpha^{*4}/(k^2 + \alpha^{*2})^2] e^{i\alpha^* r}, \quad (\text{A6})$$

where  $\alpha = (3 - 0.30)$  for the lithium 1s state with an additional 1s electron present. For the Auger initial state, one 1s state is unoccupied so that the conduction states are orthogonalized to the remaining 1s electron state, which is unscreened and has  $\alpha^* = 3.0$ . The matrix elements in this case are

$$\begin{aligned}
 f(\vec{k}, \vec{q}) &= \langle u_{1s}^B(\vec{r}) | e^{i\vec{q}\cdot\vec{r}} | u_{\vec{k}}(\vec{r}) \rangle \\
 &= 8(\pi\alpha^3)^{1/2} \frac{\alpha}{(\alpha^2 + |\vec{k} - \vec{q}|^2)^2} \\
 &\quad - \frac{8(\alpha + \alpha^*)\alpha^{*4}}{(k^2 + \alpha^{*2})^2[(\alpha + \alpha^*)^2 + q^2]^2}. \quad (A7)
 \end{aligned}$$

Again the bound-bound matrix element is partially relaxed

$$\begin{aligned}
 g(\vec{q}) &= \langle u_{1s}^B(\vec{r}) | e^{i\vec{q}\cdot\vec{r}} | u_{1s}^{B*}(\vec{r}) \rangle \\
 &= \frac{8(\alpha\alpha^*)^{3/2}(\alpha + \alpha^*)}{[(\alpha + \alpha^*)^2 + q^2]^2}. \quad (A8)
 \end{aligned}$$

Neglecting relaxation in this case means setting  $\alpha^* = \alpha = 2.70$  and neglecting orthogonalization means dropping the second term in Eq. (A7).

<sup>1</sup>J. D. Dow, J. E. Robinson, and T. R. Carver, Phys. Rev. Lett. 31, 759 (1973).

<sup>2</sup>H. W. B. Skinner, Philos. Trans. R. Soc. Lond. A 239, 95 (1940).

<sup>3</sup>A. J. McAlister, Phys. Rev. 186, 595 (1969).

<sup>4</sup>J. J. Ritsko, S. E. Schnatterly, and P. C. Gibbons, Phys. Rev. B 10, 5017 (1974).

<sup>5</sup>B. Bergersen, P. Jena, and T. McMullen, J. Phys. F 4, L219 (1974).

<sup>6</sup>G. D. Mahan, Phys. Rev. 153, 882 (1967); 163, 612 (1967).

<sup>7</sup>B. Roulet, J. Gavoret, and P. Nozières, Phys. Rev. 178, 1072 (1969); 178, 1084 (1969).

<sup>8</sup>P. Nozières and C. T. de Dominicis, Phys. Rev. 178, 1097 (1969).

<sup>9</sup>G. A. Ausman and A. J. Glick, Phys. Rev. 183, 687 (1969).

<sup>10</sup>P. Longe, Phys. Rev. B 8, 2572 (1973).

<sup>11</sup>F. K. Allotey, Phys. Rev. 157, 467 (1967).

<sup>12</sup>G. D. Mahan, Phys. Rev. B 11, 4814 (1975).

<sup>13</sup>P. Longe, Phys. Rev. B (to be published).

<sup>14</sup>P. Longe and A. J. Glick, Phys. Rev. 177, 526 (1968).

<sup>15</sup>S. M. Bose and A. J. Glick, Phys. Rev. B 10, 2733 (1974).

<sup>16</sup>B. Bergersen, T. McMullen, and J. P. Carbotte, Can. J. Phys. 49, 3155 (1971).

<sup>17</sup>L. Hedin (unpublished).

<sup>18</sup>D. R. Franceschetti and J. D. Dow, J. Phys. F. 4, L151 (1974).

<sup>19</sup>A. L. Hagen and A. J. Glick (unpublished).

<sup>20</sup>T. Kobayasi and A. Morita, J. Phys. Soc. Jpn. 28, 457 (1970).

<sup>21</sup>J. C. Slater, Phys. Rev. 36, 57 (1930).

<sup>22</sup>M. Natta and P. Joyes, J. Phys. Chem. Solids 31, 447 (1970).